Monthly Notices of the ROYAL ASTRONOMICAL SOCIETY

MNRAS **512,** L44–L48 (2022) https://doi.org/10.1093/mnrasl/slac019
Advance Access publication 2022 February 24

KiDS-1000 cosmology: machine learning – accelerated constraints on interacting dark energy with CosmoPower

A. Spurio Mancini [1]★ and A. Pourtsidou [2,3,4]

[1]*Mullard Space Science Laboratory, University College London, Holmbury St Mary, Dorking, Surrey RH5 6NT, UK*
[2]*Institute for Astronomy, The University of Edinburgh, Royal Observatory, Edinburgh EH9 3HJ, UK*
[3]*Department of Physics & Astronomy, University of the Western Cape, Cape Town 7535, South Africa*
[4]*School of Physical and Chemical Sciences, Queen Mary University of London, Mile End Road, London E1 4NS, UK*

Accepted 2022 February 21. Received 2022 February 10; in original form 2021 October 28

ABSTRACT

We derive constraints on a coupled quintessence model with pure momentum exchange from the public ∼1000 deg^2 cosmic shear measurements from the Kilo-Degree Survey and the *Planck* 2018 cosmic microwave background data. We compare this model with Lambda cold dark matter and find similar χ^2 and log-evidence values. We accelerate parameter estimation by sourcing cosmological power spectra from the neural network emulator CosmoPower. We highlight the necessity of such emulator-based approaches to reduce the computational runtime of future similar analyses, particularly from Stage IV surveys. As an example, we present Markov Chain Monte Carlo forecasts on the same coupled quintessence model for a *Euclid*-like survey, revealing degeneracies between the coupled quintessence parameters and the baryonic feedback and intrinsic alignment parameters, but also highlighting the large increase in constraining power Stage IV surveys will achieve. The contours are obtained in a few hours with CosmoPower, as opposed to the few months required with a Boltzmann code.

Key words: methods: statistical – cosmology: observations – cosmology: theory – (cosmology:) large-scale structure of the Universe.

1 INTRODUCTION

Current and forthcoming large-scale structure (LSS) surveys such as the Dark Energy Survey,[1] ESA's *Euclid* satellite mission,[2] and the Vera C. Rubin Observatory's Legacy Survey of Space and Time (VRO/LSST)[3] are aiming to probe the nature of the dark sector (dark energy and dark matter) by performing high-precision galaxy clustering and weak gravitational lensing measurements. The standard model of cosmology, Lambda cold dark matter (ΛCDM), is currently providing the best fit to a suite of data from cosmic microwave background (CMB) and LSS experiments (e.g. Anderson et al. 2012; Song et al. 2015; Beutler et al. 2016; Tröster et al. 2020; Aghanim et al. 2020b; Abbott et al. 2021; Alam et al. 2021; Heymans et al. 2021). ΛCDM assumes that dark energy is a cosmological constant, Λ, and that General Relativity describes gravity on all scales. It also assumes that dark energy and dark matter are non-interacting (uncoupled). LSS surveys are aiming to constrain exotic dark energy and modified gravity models (for reviews, see e.g. Copeland, Sami & Tsujikawa 2006; Clifton et al. 2012).

In this work, we focus on constraining interacting dark energy (IDE) in the form of a scalar field ϕ (quintessence) explicitly coupled to CDM. IDE models have been widely studied and have gained popularity as potential alternatives to ΛCDM (Amendola 2000; Pourtsidou, Skordis & Copeland 2013; Tamanini 2015; Di Valentino et al. 2020; Lucca 2021). Here, we study a subclass of models that only exhibit momentum exchange between dark energy and dark matter (Simpson 2010; Pourtsidou et al. 2013; Baldi & Simpson 2015, 2017; Amendola & Tsujikawa 2020; Chamings et al. 2020; Kase & Tsujikawa 2020). This allows them to fit CMB, supernovae, and baryon acoustic oscillation data very well (Pourtsidou & Tram 2016; Linton, Crittenden & Pourtsidou 2021), but they have not been tested yet with weak-lensing data marginalizing over baryonic feedback effects.

Baryonic and dark matter non-linear effects become particularly important in weak-lensing studies with Stage IV surveys like *Euclid* and VRO/LSST, as they dominate the small, non-linear scales with the most constraining power (Schneider et al. 2020a, b; Martinelli et al. 2021). At the same time, the computational requirements for accurate parameter estimation are becoming very expensive. A typical Markov Chain Monte Carlo requires $>10^4$ evaluations of the theoretical model under consideration, with the runtime being dominated by the computation of cosmological power spectra with Boltzmann codes such as CAMB (Lewis, Challinor & Lasenby 2000) or CLASS (Blas, Lesgourgues & Tram 2011; Lesgourgues 2011). This has led to the development of fast power spectra emulators (e.g. Aricò, Angulo & Zennaro 2021; Spurio Mancini et al. 2021; Mootoovaloo et al. 2022) to accelerate the inference pipeline by replacing the Boltzmann code at each likelihood evaluation.

★ E-mail: a.spuriomancini@ucl.ac.uk
[1] www.darkenergysurvey.org
[2] www.euclid-ec.org
[3] https://www.lsst.org/

2 MODEL

The model we study belongs to the pure momentum transfer class of theories constructed in Pourtsidou et al. (2013) and Skordis, Pourtsidou & Copeland (2015). Its main feature is that no coupling appears at the background level, regarding the fluid equations. This is in contrast to the most commonly considered coupled quintessence models, but it is also what makes this model able to fit data for a wide range of the coupling parameter β (Pourtsidou & Tram 2016). In addition, the energy-conservation equation remains uncoupled even at the linear perturbations level. Therefore, the model provides for a pure momentum-transfer coupling at the level of linear perturbations.

Following Pourtsidou & Tram (2016), we are going to concentrate on the case where the action for the scalar field ϕ is written as

$$S_\phi = \int \mathrm{d}t\, \mathrm{d}^3x\, a^3 \left[\frac{1}{2}(1-2\beta)\dot{\phi}^2 - \frac{1}{2}|\vec{\nabla}\phi|^2 - V(\phi)\right].$$

The model is physically acceptable for $\beta < \frac{1}{2}$. For $\beta \to 1/2$, there is a strong coupling pathology, while for $\beta > 1/2$, there is a ghost in the theory since the kinetic term becomes negative.

2.1 Background evolution

Assuming a flat Friedmann–Lemaître–Robertson–Walker (FLRW) universe, the background energy density and pressure for quintessence are (Pourtsidou et al. 2013)

$$\bar{\rho}_\phi = \left(\frac{1}{2}-\beta\right)\frac{\dot{\bar{\phi}}^2}{a^2} + V(\phi); \quad \bar{P}_\phi = \left(\frac{1}{2}-\beta\right)\frac{\dot{\bar{\phi}}^2}{a^2} - V(\phi), \tag{1}$$

and the energy conservation equations are the same as in uncoupled quintessence:

$$\dot{\bar{\rho}}_\phi + 3\mathcal{H}(\bar{\rho}_\phi + \bar{P}_\phi) = 0; \quad \dot{\bar{\rho}}_c + 3\mathcal{H}\bar{\rho}_c = 0. \tag{2}$$

2.2 Linear perturbations

In order to study, the observational effects of the coupled models on the CMB and LSS, we need to consider linear perturbations around the FLRW background. The density contrast $\delta_c \equiv \delta\rho_c/\bar{\rho}_c$ obeys the standard evolution equation

$$\dot{\delta}_c = -k^2\theta_c - \frac{1}{2}\dot{h}. \tag{3}$$

The momentum-transfer equation depends on the coupling parameter, β, and is given by

$$\dot{\theta}_c = -\mathcal{H}\theta_c + \frac{(6\mathcal{H}\beta\bar{Z} + 2\beta\dot{\bar{Z}})\varphi + 2\beta\bar{Z}\dot{\varphi}}{a\left(\bar{\rho}_c - 2\beta\bar{Z}^2\right)}, \tag{4}$$

where $\phi = \bar{\phi} + \varphi$ and $\bar{Z} = -\dot{\bar{\phi}}/a$. We implemented the above equations in CLASS (Blas et al. 2011; Lesgourgues 2011) in order to compute the CMB temperature and matter power spectra, following the previous implementation in Pourtsidou & Tram (2016). We fix the quintessence potential $V(\phi)$ to be the widely used single exponential form (1EXP)

$$V(\phi) = V_0 \mathrm{e}^{-\lambda\phi}. \tag{5}$$

Our initial conditions for the quintessence field are $\phi_i = 10^{-4}$, $\dot{\phi}_i = 0$. However, the same cosmological evolution is expected for a wide range of initial conditions (Copeland et al. 2006).

2.3 Non-linear effects

To exploit the constraining power of forthcoming LSS data sets on IDE models it is crucial to accurately model non-linear effects. *N*-body simulations for momentum exchange in the dark sector have been performed in Baldi & Simpson (2015, 2017), based on the elastic scattering model presented in Simpson (2010). However, for the model considered here there is no available non-linear prescription or *N*-body data. In our analysis, we employ the non-linear correction implemented in HMCODE (Mead et al. 2021), which includes modelling of baryonic feedback effects. We remark that this prescription is based on the ΛCDM model. Following Spurio Mancini et al. (2019), we justify this choice with the expected limited impact of different non-linear prescriptions on cosmological constraints from the KiDS data set, given the range of scales probed. However, this approach will need to be modified for applications to future surveys, whose dark energy constraints will strongly depend on the non-linear prescription adopted. We will return to this issue in Section 5 in the context of IDE models and discuss ways forward.

3 DATA AND METHODS

We consider the same ∼1000 deg^2 cosmic shear data from the KiDS survey (KiDS-1000) used in the recent analysis of Asgari et al. (2021, A21 in the following). Photometric redshift distributions, shear measurements and data modelling are the same presented in the KiDS-1000 papers (Giblin et al. 2021; Hildebrandt et al. 2021; Joachimi et al. 2021). As in A21, we consider three types of cosmic shear summary statistics, namely band powers (Schneider et al. 2002), Complete Orthogonal Sets of E/B-Integrals (COSEBIs; Schneider, Eifler & Krause 2010), and two-point real-space correlation functions (2PCFs).

We sample the posterior distribution using the PYTHON wrapper PYMULTINEST (Buchner et al. 2014) of the nested sampler MULTINEST (Feroz & Hobson 2008), as embedded in MONTEPYTHON (Brinckmann & Lesgourgues 2018). We compare constraints obtained running the KiDS-1000 inference pipeline (for band powers, COSEBIs and 2PCFs) and the *Planck* 2018 TTTEEE + lowE joint polarization and temperature analysis (Aghanim et al. 2020a). We use COSMOPOWER (Spurio Mancini et al. 2021, https://github.com/alessiospuriomancini/cosmopower) to replace the Boltzmann software CLASS in the computation of the matter and CMB power spectra. All contours shown in Section 4.1 have been obtained with COSMOPOWER. An accuracy comparison between COSMOPOWER and CLASS contours is reported in Section 4.2, where forecast contours are reported for a Stage IV survey configuration, obtained sourcing power spectra from CosmoPower and CLASS. The technical details of the neural network emulators are unchanged with respect to those described in Spurio Mancini et al. (2021) .

Prior distributions for the sampled parameters are the same used in A21, with the addition of two uniform distributions for the IDE parameters $\beta \sim \mathcal{U}[-0.5, 0.5]$ and $\log\lambda \sim \mathcal{U}[-3, 0.32]$. We consider a uniform prior on $\log\lambda$ to account for the fact that λ is not a dimensionless quantity (Mackay 2003). Choosing uninformative priors is crucial to avoid obtaining constraints driven by the prior assumptions (Simpson et al. 2017; Heavens & Sellentin 2018). We also report results obtained fixing λ to 1 (Copeland, Liddle & Wands 1998). The covariance matrix is the same used in A21. Its analytical computation in ΛCDM is described in Joachimi et al. (2021); we do not recompute the covariance in the IDE scenario, because similarly to Spurio Mancini et al. (2019) we expect only a weak dependence of the theoretical predictions for the observables on the IDE parameters,

Table 1. Mean and marginalized 68 per cent contours on key weak lensing parameters. We also report the χ^2 and log-Bayes factors $\log \frac{\mathcal{Z}_{\rm IDE}}{\mathcal{Z}_{\Lambda\rm CDM}}$ values. For the LSS probes the log-Bayes factors are always smaller than 0.5 in absolute value; following Jeffreys (1961), these values indicate that neither of the two models is clearly favoured with respect to the other. The *Planck* value indicates the CMB data favour the IDE model, although not in a substantial way.

	Band powers			COSEBIs			2PCFs			*Planck*		
	ΛCDM	IDE	IDE ($\lambda = 1$)	ΛCDM	IDE	IDE ($\lambda = 1$)	ΛCDM	IDE	IDE ($\lambda = 1$)	ΛCDM	IDE	IDE ($\lambda = 1$)
$\Omega_{\rm m}$	$0.341^{+0.057}_{-0.076}$	$0.342^{+0.065}_{-0.083}$	$0.343^{+0.049}_{-0.084}$	$0.314^{+0.057}_{-0.083}$	$0.315^{+0.067}_{-0.086}$	$0.318^{+0.049}_{-0.087}$	$0.269^{+0.030}_{-0.055}$	$0.272^{+0.034}_{-0.059}$	$0.270^{+0.027}_{-0.056}$	$0.320^{+0.009}_{-0.009}$	$0.318^{+0.009}_{-0.009}$	$0.335^{+0.009}_{-0.009}$
σ_8	$0.714^{+0.083}_{-0.105}$	$0.714^{+0.069}_{-0.107}$	$0.722^{+0.091}_{-0.106}$	$0.743^{+0.091}_{-0.095}$	$0.745^{+0.094}_{-0.090}$	$0.751^{+0.091}_{-0.114}$	$0.816^{+0.082}_{-0.068}$	$0.812^{+0.080}_{-0.068}$	$0.830^{+0.082}_{-0.073}$	$0.813^{+0.008}_{-0.008}$	$0.814^{+0.008}_{-0.008}$	$0.790^{+0.008}_{-0.008}$
S_8	$0.749^{+0.024}_{-0.023}$	$0.751^{+0.025}_{-0.023}$	$0.760^{+0.026}_{-0.029}$	$0.747^{+0.023}_{-0.019}$	$0.751^{+0.024}_{-0.019}$	$0.760^{+0.025}_{-0.028}$	$0.765^{+0.020}_{-0.019}$	$0.765^{+0.020}_{-0.019}$	$0.780^{+0.023}_{-0.029}$	$0.839^{+0.018}_{-0.017}$	$0.839^{+0.017}_{-0.017}$	$0.835^{+0.018}_{-0.015}$
χ^2	148.0036	148.2647	148.7240	77.9787	77.5061	78.4702	255.4080	256.4388	254.7876	980.7286	980.7316	980.5730
$\log \frac{\mathcal{Z}_{\rm IDE}}{\mathcal{Z}_{\Lambda\rm CDM}}$		-0.055 ± 0.144	-0.240 ± 0.140		0.136 ± 0.146	-0.048 ± 0.148		-0.048 ± 0.183	0.151 ± 0.184		0.980 ± 0.277	0.402 ± 0.279

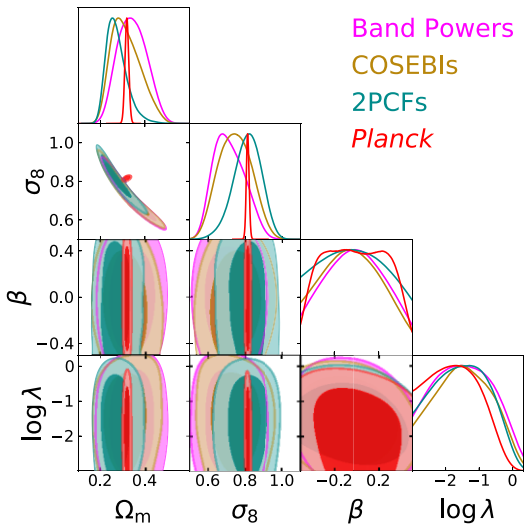

Figure 1. 68 and 95 per cent marginalized contours for key weak lensing parameters $\Omega_{\rm m}$, σ_8, S_8, and the IDE parameters β, λ. Contours for band powers, COSEBIs and two-point correlation functions are shown in magenta, brown, and cyan, respectively, while *Planck* contours in red.

verified by the weak constraints obtained on these parameters (see Section 4.1).

4 RESULTS

4.1 Constraints from KiDS-1000 and *Planck*

Fig. 1 shows a comparison of marginalized 68 and 95 per cent contours of the posterior distribution for the key parameters $\Omega_{\rm m}$, σ_8, and $S_8 = \sigma_8\sqrt{\Omega_{\rm m}/0.3}$, as well as for the IDE parameters β, λ. As expected, the latter are unconstrained: differences in the matter power-spectrum predictions for IDE models with respect to ΛCDM are mostly significant at highly non-linear scales, only very mildly probed by the KiDS-1000 data. The *Planck* likelihood does not constrain β and λ either, in agreement with the fact that the CMB power spectra are essentially insensitive to these parameters, except on very large, cosmic variance-dominated scales (Pourtsidou & Tram 2016).

Table 1 shows the numerical values of the mean and 68 per cent credibility intervals for $\Omega_{\rm m}$, σ_8, and S_8, along with χ^2 and log-evidence values, for all cosmic shear summary statistics as well as for *Planck*. Fig. 2 shows contours on the $\Omega_{\rm m}$–S_8 plane for the ΛCDM and IDE scenarios. The latter is analysed varying both β and λ, as well as setting $\lambda = 1$. With this last choice we find an attenuation of the tension up to $\sim 1\sigma$. In Table 1, the χ^2 and log-evidence values for ΛCDM and IDE scenarios (both varying and fixing λ) are similar across all three summary statistics, hence neither of the two cosmological models is clearly favoured over the other, although the *Planck* data seem to mildly prefer the IDE model over ΛCDM. Future analyses from Stage IV surveys will have the constraining power to provide stronger model comparison statements. It will be interesting to explore larger prior ranges for β, as well as different coupling functions, which may lead to stronger alleviation of the S_8 tension. For the KiDS-1000 data used in this paper we verified that larger, negative values of β do not help alleviate the S_8 tension.

4.2 Forecasts for a *Euclid*-like survey

In Fig. 3, we present forecast contours for a *Euclid*-like Stage IV survey. The simulated configuration is the same presented in Spurio Mancini et al. (2019), including the prior distributions on cosmological and astrophysical nuisance parameters. For the IDE parameters β and λ, we use prior distributions $\beta \sim \mathcal{U}[-0.5, 0.5]$ and $\lambda \sim \mathcal{U}[0., 2.1]$. We note that the prior on λ differs from the one used for the KiDS-1000 data; for future analyses of real data from e.g. *Euclid*, it will be important to consider a uniform prior on $\log\lambda$ to account for the fact that λ is not a dimensionless quantity (Mackay 2003). Here, the goal is to highlight the importance of emulator-based approaches such as the one presented in this paper and based on COSMOPOWER. With this emulator, we obtained the contours for the *Euclid*-like survey (in *blue* in Fig. 3) in $\sim$ 9 h running on 48 cores. For comparison, sourcing power spectra from the Boltzmann code CLASS required a runtime of $\sim$ 5 months on the same hardware configuration (red contours in Fig. 3).

We note that this Stage IV survey configuration leads to much stronger constraints on IDE parameters β and λ, namely $\beta = -0.001^{+0.023}_{-0.024}$ and $\lambda = 1.231^{+0.054}_{-0.051}$ (68 per cent contours). We also see that these IDE parameters are degenerate with nuisance parameters $A_{\rm IA}$ and $\eta_{\rm IA}$, modelling amplitude and redshift dependence of the intrinsic alignment signal, respectively, as well as the HMCODE parameters $c_{\rm min}$ and η_0, describing minimum halo concentration and halo bloating, respectively. These degeneracies highlight the importance of developing accurate prescriptions for non-linearities and systematics that can guarantee unbiased constraints on dark energy.

5 CONCLUSIONS

We presented constraints on an IDE model from $\sim$1000 deg^2 cosmic shear measurements from the Kilo-Degree Survey (KiDS-1000). A comparison with *Planck* measurements of the CMB shows an alleviation up to $\sim 1\sigma$ of the tension in the parameter $S_8 = \sigma_8\sqrt{\Omega_{\rm m}/0.3}$, with respect to the $\sim 3\sigma$ tension of the ΛCDM analysis of Asgari et al. (2021). Constraints on the IDE model were obtained taking

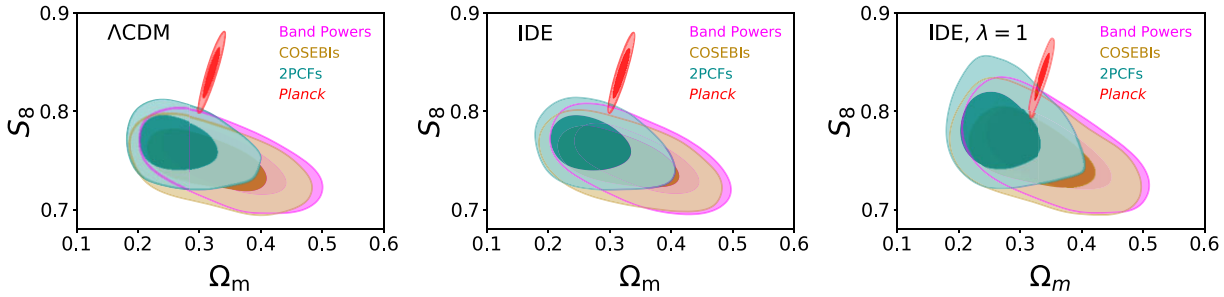

Figure 2. 68 and 95 per cent marginalized contours in the $\Omega_m - S_8$ plane. The colour code is the same as in Fig. 1.

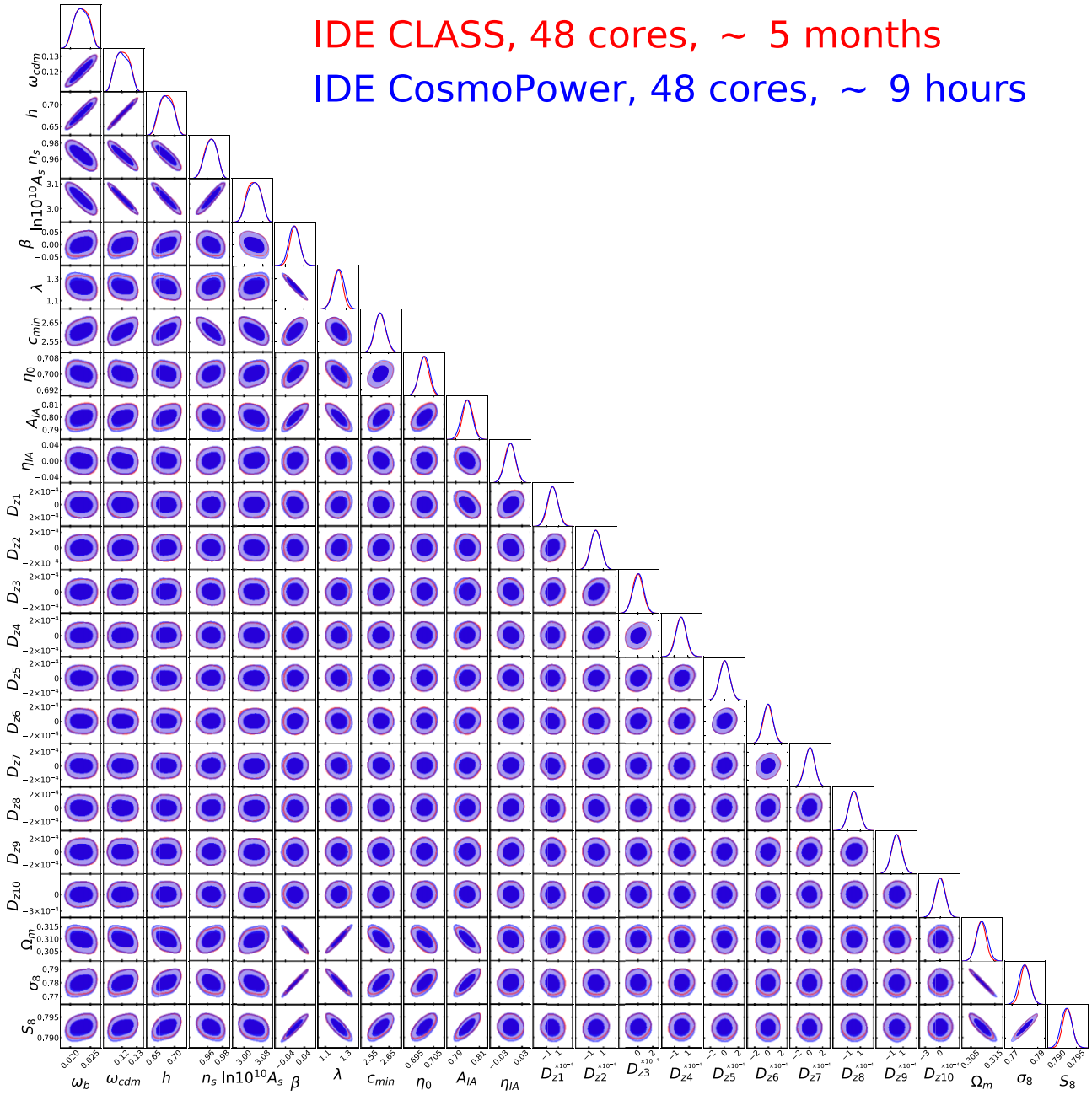

Figure 3. Forecasts for a *Euclid*-like survey. The meaning of each parameter is explained in Spurio Mancini et al. (2021), whose analysis set-up is identical to that considered here, with the sole addition of the IDE parameters β and λ, introduced in Section 2.

into account, for the first time, baryonic feedback effects. Given the absence of bespoke non-linear prescriptions for IDE models, we adopted the ΛCDM-based non-linear prescription implemented in the software HMCODE. For applications to future surveys, proper non-linear prescriptions for IDE models will need to be developed. We plan to consider the Elastic Scattering model and the *halo model reaction* framework (Cataneo et al. 2019; Bose et al. 2020; Tröster et al. 2021) for this purpose.

In deriving constraints, we used the neural network-based emulator of cosmological power spectra COSMOPOWER to accelerate the inference pipeline. We highlight the importance of such emulator-based approaches, in particular for applications to Stage IV surveys analyses. To demonstrate this point, we performed a forecast for a Stage IV *Euclid*-like survey for the same IDE model constrained with the KiDS-1000 data. Sourcing power spectra from COSMOPOWER allowed us to obtain contours in a few hours, while the same contours obtained using a Boltzmann code required a few months of run time.

The emulators trained for this analysis will remain available. For example, following Spurio Mancini et al. (2021), we emulated the linear matter power spectrum and a non-linear boost. As new, bespoke non-linear corrections for IDE models become available, the COSMOPOWER emulator for the non-linear boost can be trained on them, while for the linear power spectrum we can reuse the emulator trained for this analysis.

ACKNOWLEDGEMENTS

We thank B. Joachimi and A. Mead for comments on the manuscript, and S. Brieden and T. Tram for useful discussions. We thank the anonymous referee for their valuable review of the paper. ASM is supported by the MSSL STFC Consolidated Grant. AP is a UK Research and Innovation Future Leaders Fellow (grant MR/S016066/1). This work used facilities provided by the UCL Cosmoparticle Initiative. We acknowledge the use of GETDIST (Lewis et al. 2000) to obtain corner plots. Based on observations made with ESO Telescopes at the La Silla Paranal Observatory under programme IDs 177.A-3016, 177.A-3017, 177.A-3018, and 179.A-2004, and on data products produced by the KiDS consortium. The KiDS production team acknowledges support from Deutsche Forschungsgemeinschaft, ERC, NOVA, and NWO-M grants; Target; and the University of Padova and the University Federico II (Naples). We used the gold sample of weak lensing and photometric redshift measurements from the fourth data release of the Kilo-Degree Survey (Kuijken et al. 2019; Wright et al. 2020; Hildebrandt et al. 2021; Giblin et al. 2021), referred to as KiDS-1000. Cosmological parameter constraints from KiDS-1000 have been presented in Asgari et al. (2021) (cosmic shear), Heymans et al. (2021) (3 × 2pt), and Tröster et al. (2021) (beyond ΛCDM), with the methodology presented in Joachimi et al. (2021). Based on observations obtained with Planck (http://www.esa.int/Planck), an ESA science mission with instruments and contributions directly funded by ESA Member States, NASA, and Canada.

DATA AVAILABILITY

KiDS-1000 data are available at http://kids.strw.leidenuniv.nl/DR4/lensing.php. The emulators used in this analysis are shared on the COSMOPOWER GitHub repository .

REFERENCES

Abbott T. M. C. et al., 2022, Physical Review D, 105
Aghanim N. et al., 2020a, A&A, 641, A5
Aghanim N. et al., 2020b, Astron. Astrophys., 641, A6
Alam S. et al., 2021, Phys. Rev. D, 103, 083533
Amendola L., 2000, Phys. Rev., D62, 043511
Amendola L., Tsujikawa S., 2020, JCAP, 06, 020
Anderson L. et al., 2012, MNRAS, 427, 3435
Aricò G., Angulo R. E., Zennaro M., 2021, preprint (arXiv:2104.14568)
Asgari M. et al., 2021, A&A, 645, A104
Baldi M., Simpson F., 2015, MNRAS, 449, 2239
Baldi M., Simpson F., 2017, MNRAS, 465, 653
Beutler F. et al., 2016, MNRAS, 466, 2242
Blas D., Lesgourgues J., Tram T., 2011, JCAP, 07, 034
Bose B., Cataneo M., Tröster T., Xia Q., Heymans C., Lombriser L., 2020, MNRAS, 498, 4650
Brinckmann T., Lesgourgues J., 2018, preprint (arXiv:1804.07261)
Buchner J. et al., 2014, A&A, 564, A125
Cataneo M., Lombriser L., Heymans C., Mead A., Barreira A., Bose S., Li B., 2019, MNRAS, 488, 2121
Chamings F. N., Avgoustidis A., Copeland E. J., Green A. M., Pourtsidou A., 2020, Phys. Rev. D, 101, 043531
Clifton T., Ferreira P. G., Padilla A., Skordis C., 2012, Phys. Rep., 513, 1
Copeland E. J., Liddle A. R., Wands D., 1998, Phys. Rev. D, 57, 4686
Copeland E. J., Sami M., Tsujikawa S., 2006, Int. J. Mod. Phys. D, 15, 1753
Di Valentino E., Melchiorri A., Mena O., Vagnozzi S., 2020, Phys. Rev. D, 101, 063502
Feroz F., Hobson M. P., 2008, MNRAS, 384, 449
Giblin B. et al., 2021, A&A, 645, A105
Heavens A. F., Sellentin E., 2018, J. Cosmol. Astropart. Phys., 2018, 047
Heymans C. et al., 2021, A&A, 646, A140
Hildebrandt H. et al., 2021, A&A, 647, A124
Jeffreys S. H., 1961, Theory of Probability, 3rd edn., Oxford
Joachimi B. et al., 2021, A&A, 646, A129
Kase R., Tsujikawa S., 2020, JCAP, 11, 032
Kuijken K. et al., 2019, A&A, 625, A2
Lesgourgues J., 2011, preprint (arXiv:1104.2932)
Lewis A., Challinor A., Lasenby A., 2000, ApJ, 538, 473
Linton M. S., Crittenden R., Pourtsidou A., 2021, preprint (arXiv:2107.03235)
Lucca M., 2021, Phys. Dark Univ., 34, 100899
Mackay D. J. C., 2003, Information Theory, Inference and Learning Algorithms. Cambridge University Press, New York
Martinelli M. et al., 2021, Astron. Astrophys., 649, A100
Mead A. J., Brieden S., Tröster T., Heymans C., 2021, MNRAS, 502, 1401
Mootoovaloo A., Jaffe A. H., Heavens A. F., Leclercq F., 2022, Astron. Comput., 38, 100508
Pourtsidou A., Tram T., 2016, Phys. Rev. D, 94, 043518
Pourtsidou A., Skordis C., Copeland E., 2013, Phys. Rev. D, 88, 083505
Schneider A. et al., 2020b, JCAP, 04, 020
Schneider P., van Waerbeke L., Kilbinger M., Mellier Y., 2002, A&A, 396, 1
Schneider P., Eifler T., Krause E., 2010, Astron. Astrophys., 520, A116
Schneider A., Stoira N., Refregier A., Weiss A. J., Knabenhans M., Stadel J., Teyssier R., 2020a, JCAP, 04, 019
Simpson F., 2010, Phys. Rev. D, 82, 083505
Simpson F., Jimenez R., Pena-Garay C., Verde L., 2017, J. Cosmol. Astropart. Phys., 2017, 029
Skordis C., Pourtsidou A., Copeland E., 2015, Phys. Rev. D, 91, 083537
Song Y.-S. et al., 2015, Phys. Rev. D, 92, 043522
Spurio Mancini A. et al., 2019, MNRAS, 490, 2155
Spurio Mancini A., Piras D., Alsing J., Joachimi B., Hobson M. P., MNRAS, 2022, 511, 1771
Tamanini N., 2015, Phys. Rev. D, 92, 043524
Tröster T. et al., 2020, Astron. Astrophys., 633, L10
Tröster T. et al., 2021, Astron. Astrophys., 649, A88
Wright A. H., Hildebrandt H., van den Busch J. L., Heymans C., 2020, A&A, 637, A100

This paper has been typeset from a TEX/LATEX file prepared by the author.